



## Novel hexahydropyrrolo[3,4-c]pyrrole CCR5 antagonists

David M. Rotstein\*, Chris R. Melville, Fernando Padilla, Dick Cournoyer, Eun K. Lee, Remy Lemoine, Ann C. Petersen, Lina Q. Setti, Jutta Wanner, Lijing Chen, Lubov Filonova, David G. Loughhead, Jason Manka, Xiao-Fa Lin, Shelley Gleason, Surya Sankuratri, Changhua Ji, Andre deRosier, Marianna Dioszegi, Gabrielle Heilek, Andreas Jekle, Pamela Berry, Cheng-I Mau, Paul Weller

Roche Palo Alto LLC, 3431 Hillview Avenue, Palo Alto, CA 94304, USA

### ARTICLE INFO

#### Article history:

Received 26 February 2010

Revised 23 March 2010

Accepted 26 March 2010

Available online 30 March 2010

#### Keywords:

CCR5 antagonist

Chemokine

Anti-HIV-1

Antiviral

### ABSTRACT

Starting with a high-throughput screening lead, a novel series of CCR5 antagonists was developed utilizing an information-based approach. Improvement of pharmacokinetic properties for the series was pursued by SAR exploration of the lead template. The synthesis, SAR and biological profiles of the series are described.

© 2010 Elsevier Ltd. All rights reserved.

Despite remarkable advances in the treatment of HIV/AIDS, a major challenge is the rapid evolution of resistant viral strains. Thus, there remains a need for the development of new therapeutic agents.<sup>1</sup> As one of the two key co-receptors for HIV entry, blockade of CCR5 continues to be an area of therapeutic interest.<sup>2</sup> In a continuation of our efforts towards the discovery of CCR5 antagonists for the treatment of HIV/AIDS<sup>3</sup> and potentially for a variety of autoimmune indications,<sup>4</sup> studies of new, novel templates were pursued.

Examination of hits from high-throughput screening of the Roche library versus the CCR5 receptor revealed compound **1** as a low potency antagonist. Comparison of this hit to the Pfizer clinical candidate, maraviroc **2**,<sup>5</sup> suggested that the hexahydropyrrolo[3,4-c]pyrrole group present in **1** might serve as a bioisostere for the tropane subunit in maraviroc. A similar comparison to the Schering series of CCR5 antagonists,<sup>6</sup> represented by structure **3**, suggested replacement of the dichlorobenzyl group of **1** with the 2,6-dimethyl benzamide group of **3**. Figure 1 illustrates this strategy and the first example of our morphed template, compound **4**.

As can be seen in Table 1, compound **4** demonstrated excellent binding and antiviral activity with IC<sub>50</sub> values of 6 and 7 nM, respectively. These are comparable to both Pfizer's maraviroc **2** (binding and antiviral IC<sub>50</sub> of 14 and 3 nM, respectively) and Schering analog **3** (binding and antiviral IC<sub>50</sub> of 6 and 4 nM, respectively).<sup>7</sup>

A major issue to be addressed with this lead compound was the high intrinsic clearances observed in human (HLM) and rat (RLM) liver microsomes: 256 and 312 μl/min/mg, respectively.<sup>8</sup> These in vitro values corresponded to projected in vivo clearances close to hepatic blood flow.<sup>9</sup> Subsequent rat PK experiments were

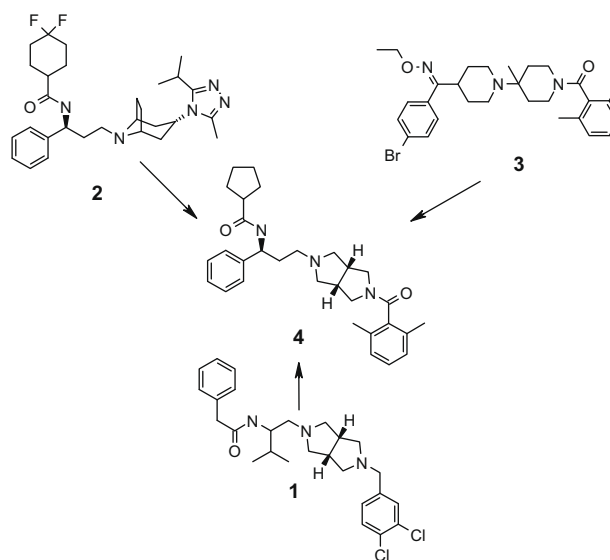
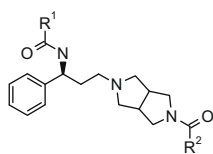


Figure 1.

\* Corresponding author. Tel.: +1 408 7329030.

E-mail address: [david.rotstein@comcast.net](mailto:david.rotstein@comcast.net) (D.M. Rotstein).

**Table 1**  
Tail SAR of lead compound **4**

#	R <sup>1</sup>	R <sup>2</sup>	Binding <sup>a</sup> IC <sub>50</sub>	Antiviral <sup>b</sup> IC <sub>50</sub>
<b>4</b>			6	7
<b>5</b>	CH <sub>3</sub>		15	132
<b>6</b>			11	100
<b>7</b>			7	39
<b>8</b>			3	30
<b>9</b>			4	9
<b>10</b>			8	124
<b>11</b>			18	85
<b>12</b>			15	101

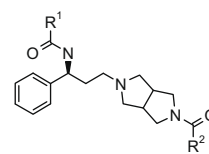
<sup>a</sup> Competitive binding evaluated versus RANTES with IC<sub>50</sub> values in nM, as mean of two experiments.

<sup>b</sup> Antiviral IC<sub>50</sub> values in nM as mean of two experiments.

consistent with this projection: only 3% bioavailability was obtained upon PO dosing at 10 mg/kg. Thus, a SAR study of this template was initiated, seeking to improve our lead's DMPK characteristics, while maintaining good antiviral activity.

In describing results from our studies, the cyclopentyl and benzamide groups are typically referred to as the tail and head groups of the template, respectively. In our series, as has previously observed,<sup>10</sup> good antagonist binding to the CCR5 receptor was maintained across a range of structural modifications. In contrast, antiviral potency in cells was more sensitive to structural changes. Initial SAR studies of the tail group show a preference for cyclic aliphatic rings. As seen in Table 1, replacement of the cyclopentyl tail group with methyl or isopropyl, as in **5** and **6**, led to significant loss in antiviral potency. Shrinkage of cyclopentyl to cyclobutyl or enlargement to cyclohexyl (analogs **7** and **8**) led to ~5-fold loss in antiviral activity. However, incorporation of a 4,4-difluorocyclohexyl tail restored antiviral activity as seen with analog **9**. Compounds **10–12** demonstrate that aryl, heteroaryl and heterocycle functionalities were not well tolerated in the tail region. Metabolic stability assessment of analogs from Table 1 showed no improvement in intrinsic clearance (data not shown).

Table 2 describes results from studies of head group SAR. Deletion of the benzamide group, as in acetyl analog **13**, resulted in complete loss of binding and antiviral activity. Removal of either or both of the 2,6-dimethyl flanking groups gave a similar result (data not shown), however, replacement with halogen was tolerated as can be seen with compound **14**. The 2,6-dichloro analog **15** maintained binding activity but lost significant antiviral potency. Additional 4-substitution on the aryl ring was tolerated, as demonstrated by 4-fluoro and 4-methoxy analogs (**16** and **17**). Aryl replacement with a five member heteroaromatic such as isoxazole **18**, resulted in a loss of antiviral activity. A variety of six member

**Table 2**  
Head SAR of lead compound **4**

#	clog P	R <sup>1</sup>	R <sup>2</sup>	Binding IC <sub>50</sub> <sup>a</sup>	Antiviral IC <sub>50</sub> <sup>a</sup>	HLM/RLM <sup>b</sup>	Caco <sup>c</sup> AB/ER
<b>4</b>	4.7			6	7	256/322	4/5
<b>13</b>	2.1		Me	465	>1000	ND	ND
<b>14</b>	5			9	3	264/ND	ND
<b>15</b>	5.2			14	92	389/ND	ND
<b>16</b>	5			6	3	236/517	ND
<b>17</b>	5			26	0.4	241/236	33/2
<b>18</b>	2.8			19	545	ND	ND
<b>19</b>	3.6			7	7	67/89	4/17
<b>20</b>	2.3			44	19	6/12	.1/300
<b>21</b>	2.7			14	27	35/51	1.3/17
<b>22</b>	2.5			30	6	25/25	0.5/5
<b>23</b>	3.4			12	0.4	227/144	3/8

<sup>a</sup> Defined as in Table 1.

<sup>b</sup> Human liver microsomal intrinsic clearance (μl/min/mg protein).

<sup>c</sup> Permeability in Caco-2 cells (cm/sec × 10E<sup>-6</sup>) apical to basolateral (AB) and basolateral to apical (BA) movement of test compound in 21-day cultured Caco-2 cells. ER = efflux ratio of BA to AB.

heteroaromatic rings such as pyridine, pyridine *N*-oxide, pyrimidine, pyridone and 6-cyanopyridine maintained good activity (**19–23**). Another beneficial feature of these more polar analogs is that the heteroatom substitution improved metabolic stability by lowering overall lipophilicity and blocking specific sites of metabolism. However, a downside of the decreased lipophilicity is that, in general, the resultant molecules demonstrated decreased permeability and enhanced efflux in Caco-2 cells (contrast analogs **4** vs **19** and **20**).

A number of these analogs were screened to assess their in vivo PK in rat. As can be seen in Table 3, the increased metabolic stability of analogs such as **19** and **21** resulted in somewhat improved bioavailability relative to our starting point with compound **4**. However, no effect was seen on the high systemic clearance as the structural modifications have not addressed the primary driver of clearance, Pgp mediated efflux.

Additional SAR studies were performed around advanced lead **21** to address these DMPK issues and optimize potency. As can

**Table 3**  
Pharmacokinetic profile in rat<sup>a</sup>

Compd #	AUC PO (ng·h/mL)	Cl IV (mL/min/kg)	%F
<b>4</b>	31	134	2.7
<b>19</b>	65	151	6.4
<b>21</b>	309	131	17

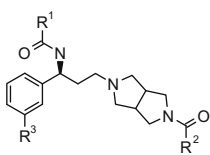
<sup>a</sup> Doses were 1 mg/kg IV and 10 mg/kg PO, AUC and %F were determined after the oral dose and Cl was determined from the IV dose.

be seen in Table 4, replacement of the cyclopentyl tail of **21**, with 4,4-difluoro cyclohexyl or 3,3-difluorocyclobutyl afforded analogs **24** and **25**, both of which showed improved antiviral activity, but at a cost of microsomal stability. Substitution of a 3-fluoro or 3-chloro on the phenyl tail also increased antiviral potency (**26–29**). However, the 3,5-difluorophenyl or 3-cyanophenyl analogs, **30–31**, showed decreased antiviral activity.

As detailed in Table 5, screening of analogs **24** and **28** in rat PK failed to show significant improvement in exposure. Interestingly, when these compounds were administered to dogs, much improved exposure was observed compared to rat despite similar intrinsic microsomal stabilities (DLM clearance is 30 and 15 µl/min/mg, respectively, for **24** and **28**). One potential explanation for this difference is the increased contribution of paracellular absorption through the larger pore junctions in the dog gastrointestinal tract.

An example of the synthetic route utilized to prepare our series, the synthesis of analog **4**, is shown in Scheme 1.<sup>11</sup>

A [2,3]-dipolar cycloaddition between *N*-benzylmaleimide **32** and the imine ylide derived from *N*-benzylglycine **33** and

**Table 4**  
Tail SAR of lead compound **21**


#	R <sup>1</sup>	R <sup>2</sup>	R <sup>3</sup>	Binding IC <sub>50</sub> <sup>a</sup>	Antiviral IC <sub>50</sub> <sup>a</sup>	HLM/RLM
<b>21</b>			H	14	27	35/51
<b>24</b>			H	27	6	83/46
<b>25</b>			H	20	3	60/61
<b>26</b>			3-Fl	13	3.6	129/17
<b>27</b>			3-Fl	12	1.1	113/24
<b>28</b>			3-Fl	9	0.8	28/29
<b>29</b>			3-Cl	25	2	182/111
<b>30</b>			3,5-Di-Fl	30	41	45/ND
<b>31</b>			3-CN	34	203	30/31

<sup>a</sup> Defined as in Tables 1 and 2.

**Table 5**  
Pharmacokinetic profile in rat and dog

Pharmacokinetics <sup>a</sup>	<b>24</b>	<b>28</b>
Rat AUC (ng h/mL)	215	108
Rat Cl (ml min/kg)	99	105
Rat %F	15	18
Dog AUC (ng h/mL)	4210	307
Dog Cl (ml min/kg)	44	36
Dog %F	103	72

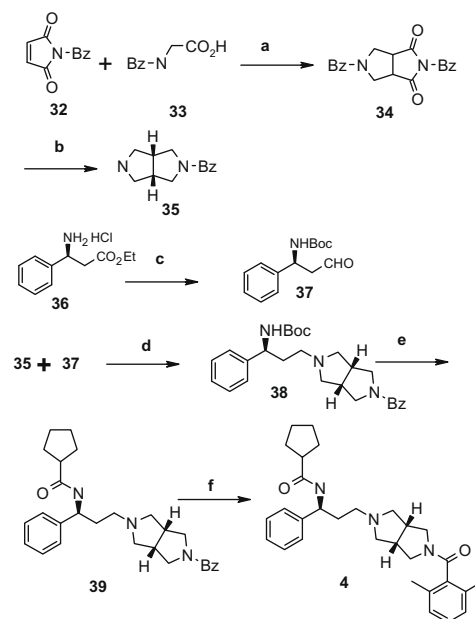
<sup>a</sup> IV/PO doses 1/10 mg/kg except for compound **28** in dog where IV/PO doses were 1/1 mg/kg. AUC and %F were determined after the oral dose and Cl was determined from the IV dose.

paraformaldehyde gave 2,5-dibenzyltetrahydropyrrolo[3,4-c]pyrrole-1,3-dione **34**. Selective debenzylation with 1-chloroethyl chloroformate, followed by imide reduction with lithium aluminum hydride afforded 2-benzylcyclopentane-1,3-dione **35**.

((*S*)-3-Oxo-1-phenylpropyl)-carbamic acid *tert*-butyl ester **37** was prepared by BOC protection of (*S*)-3-amino-3-phenylpropionic acid ethyl ester **36** using BOC anhydride, followed by chemoselective reduction of the ester to the corresponding aldehyde **37**.

Reductive amination of amine **35** with aldehyde **37** using sodium triacetoxyborohydride gave intermediate **38**. BOC removal with HCl was followed by amide coupling with cyclopentanecarboxylic acid, EDCl, HOBT and diisopropylethylamine to yield **39**. Debenzylation of **39** under catalytic hydrogenolysis conditions afforded the respective amine, which was followed by amide formation with 2,6-dimethylbenzoic acid to afford the desired product, cyclopentanecarboxylic acid ((*S*)-3-[5-(2,6-dimethylbenzoyl)hexahydropyrrolo[3,4-c]pyrrol-2-yl]-1-phenylpropyl)amide, **4**.

In summary, building from an in-house lead, an information-based approach led to the rapid discovery of a series of novel CCR5 antagonists with potent antiviral activity. Extensive SAR studies afforded analogs with improved in vitro and in vivo DMPK properties.



**Scheme 1.** Reagents and conditions: (a) (CH<sub>2</sub>O)<sub>n</sub>, toluene, reflux, 86%; (b) (i) 1-chloroethyl chloroformate, CH<sub>2</sub>Cl<sub>2</sub>, reflux, 91%, (ii) LAH, THF, 70 °C, 95%; (c) (i) NaOH, (BOC)<sub>2</sub>O, H<sub>2</sub>O, THF, (ii) DIBAL, CH<sub>2</sub>Cl<sub>2</sub>, -78 °C, 87%; (d) sodium triacetoxyborohydride, CH<sub>2</sub>Cl<sub>2</sub>, rt, 88%; (e) (i) HCl, MeOH, 50 °C, (ii) cyclopentanecarboxylic acid, EDCl, HOBT, *i*-Pr<sub>2</sub>NEt, CH<sub>2</sub>Cl<sub>2</sub>, rt, 94% for two steps; (f) (i) ammonium carbonate, Pd(OH)<sub>2</sub>, EtOH, reflux, (ii) 2,6-dimethylbenzoic acid, EDCl, HOBT, *i*-Pr<sub>2</sub>NEt, CH<sub>2</sub>Cl<sub>2</sub>, 56% for two steps.

## Acknowledgements

The authors thank Gary Cooper, Felicia Thai, Bill Bingenheimer and Eric Humphreys for synthetic support; Rama Kondru, Nidhi Arora and Taraneh Mirzadegan for computational support; Yanzhou Liu for expert NMR analysis; Marquis L. Cummings Jr. for chiral HPLC purifications; Naina Patel for formulation development; Joe Muchowski, Counde Oyang, David Goldstein, David Swinney, Denis Kertesz and Eric Sjogren for helpful discussions.

## References and notes

1. Perno, C.-F.; Moyle, G.; Tsoukas, C.; Ratanasuwan, W.; Gatell, J.; Schechter, M. *J. Med. Virol.* **2008**, *80*, 565.
2. Palani, A.; Tagat, J. R. *J. Med. Chem.* **2006**, *49*, 2851.
3. Rotstein, D. M.; Gabriel, S. D.; Makra, F.; Filonova, F.; Gleason, S.; Brotherton-Pleiss, C.; Setti, L. Q.; Trejo-Martin, A.; Lee, E. K.; Sankuratri, S.; Ji, C.; de Rosier, A.; Dioszegi, M.; Heilek, G.; Jekle, A.; Berry, P.; Weller, P.; Mau, C.-I. *Bioorg. Med. Chem. Lett.* **2009**, *19*, 5401.
4. Turner, J. E.; Steinmetz, O. M.; Stahl, R. A.; Panzer, U. *Mini-Rev. Med. Chem.* **2007**, *7*, 1089.
5. MacArthur, R. D.; Novak, R. M. *Rev. Anti-Infect. Agents* **2008**, *47*, 236.
6. Palani, A.; Shapiro, S.; Clader, J. W.; Greenlee, W. J.; Cox, K.; Strizki, J.; Endres, M.; Baroudy, B. M. *J. Med. Chem.* **2001**, *44*, 3339.
7. Briefly, for the antiviral assay, pseudo-type particles were generated by co-transfection of envelope deleted HIV-1 genomic plasmid (derived from pNL4-3) and an envelope expression plasmid carrying viral envelope from NL-Bal into 293T cells. Culture supernatant containing pseudo-typed viruses was harvested after 2 days and used to infect JC53-BL reporter cells. Luciferase reporter gene activity was measured 3 days post-infection. For more detailed assay protocols see: Melville, C.R.; Rotstein, D.M. WO2008119663.
8. The thresholds above which intrinsic microsomal clearance values were considered to be high were  $\geq 90$   $\mu\text{l}/\text{min}/\text{mL}$  for RLM and  $\geq 35$   $\mu\text{l}/\text{min}/\text{ml}$  for HLM. These scaled to in vivo clearance values  $\geq 70\%$  of liver blood flow using the well-stirred model. Intrinsic microsomal clearance values corresponding to  $\leq 30\%$  of liver blood flow ( $\leq 15$   $\mu\text{l}/\text{min}/\text{ml}$  for RLM and  $\leq 6.5$   $\mu\text{l}/\text{min}/\text{ml}$  for HLM) were considered to be low.
9. Obach, R. S. *Curr. Opin. Drug Discovery Dev.* **2001**, *4*, 36.
10. Ernst, J.; Dahl, R.; Lum, C.; Urban, J.; Miller, S. G.; Lundström J. *Bioorg. Med. Chem. Lett.* **2008**, *18*, 1498.
11. For more detailed experimental information, see: Lee, E.K.; Melville, C. R.; Rotstein, D.M. WO2005121145.